

Innovative Design for Mutual Coupling Reduction in Dual-Element Array Antennas for ISM Applications Using Whale Optimization Algorithm

Elham Atashpanjeh and Pejman Rezaei*

Department of Electrical and Computer Engineering, Semnan University, Semnan, Postal Code: 35131-19111, Iran

ABSTRACT: This paper introduces a decoupled dual-element array antenna designed to address the challenges of mutual coupling between elements. To tackle this issue, a neutralization line is strategically incorporated to suppress leaky surface currents, while ensuring that the antenna's central frequency and radiation pattern remain intact. The dimensions of the neutralization line are carefully optimized using the Whale Optimization Algorithm (WOA) to achieve the best possible performance, focusing on minimizing mutual coupling and enhancing gain. By placing the neutralization line nearby between the two elements, surface currents are efficiently redirected back to the radiating element, preventing leakage to neighboring elements. This approach also results in a more compact structure. The proposed antenna, with overall dimensions of $50 \text{ mm} \times 30 \text{ mm} \times 1.6 \text{ mm}$, is simulated using analytic software. It achieves an impressive 27 dB reduction in mutual coupling and delivers an ultra-wide bandwidth of 1.2 GHz within the Industrial Scientific and Medical (ISM) band at an operating frequency of 2.4 GHz, with a measured maximum gain of -5.19 dB . The structure was fabricated, and experimental results closely matched the simulations, confirming the design's effectiveness. By leveraging the WOA optimization method, the geometry of the neutralization line was fine-tuned to maximize performance, significantly improving inter-element decoupling. This design approach is simple yet effective and can be readily extended to other antenna array configurations, demonstrating strong potential for compact and efficient ISM band applications.

1. INTRODUCTION

Significant growth has been observed in the utilization of Multiple-Input Multiple-Output (MIMO) techniques with Ultra-Wideband (UWB) array antennas since the 1970s, attributed to the increasing demand for high-speed wireless communication systems and Internet of Things (IoT) devices [1–5]. Under this development, microstrip antennas have emerged as a preferred choice for MIMO configurations due to their special features and adaptability, as explained with integrated filters in [6, 7]. These antennas offer several benefits such as miniaturized size, ease of integration with circuitry, and compatibility with diverse substrates, making them suitable for various MIMO applications [8]. The attainment of compact components is emphasized as the primary and critical necessity. This requirement arises due to the need for space-efficient designs in different applications. Additionally, the presence of the Mutual Coupling (MC) phenomenon is highlighted as a significant concern. This phenomenon refers to the interaction between closely spaced antennas within an array, which can lead to undesired effects such as reduced antenna performance and distorted radiation patterns. These challenges become particularly pronounced in densely packed array antennae, where the proximity of elements intensifies the MC effects [9]. It should be noted that the coupling between the elements of an antenna can be useful in the design of the required structure, such as the mul-

tilayered patch microstrip antenna [10], but in this article, the coupling between the elements in an array is considered. Moreover, the implementation of specialized fractal geometries, such as the slot and Slotted Patch Radiator (SPR)-loaded four-port hen-shaped fractal UWB-MIMO antenna, further illustrates advanced approaches in managing coupling while maintaining compact design [11, 12]. It is worth noting that based on experimental results, it becomes evident that when the distance between antennas is less than $\frac{\lambda_0}{2}$, the radiation parameters of the antennas are significantly influenced by surface waves and near-field coupling effects between adjacent antennas [13–15]. In MIMO systems, the compact nature inherently presents challenges in increasing the distances between constituent elements to reduce cross-coupling issues. For this reason, a solution for reducing MC in patch array antennas is proposed in [16]. In this work, an arrangement of metallic walls and shorting pins was employed to address this issue. Another approach, detailed in [17], introduces the utilization of plane spiral orbital angular momentum electromagnetic waves for mitigating MC in an array antenna. In order to address the challenge of MC between antennas, various decoupling techniques have been proposed in the literature. The decoupling techniques are classified into two key classifications: structural approaches and network-based methods. Structural approaches involve the selection of antennas, as well as their positioning and alignment. On the other hand, network-based methods typically rely on analytical approaches utilizing network parameters and matrix

* Corresponding author: Pejman Rezaei (prezaei@semnan.ac.ir).

operations [18, 19]. Here, some references are cited that have addressed the mitigation of MC issues through structural approaches. For instance, [20] introduces a novel topology for a differential negative group delay circuit, leveraging a reverse nested double U-formed DGS (Defected Ground Structure). This approach offers promise in mitigating MC effects. Moreover, a flexible design method for microstrip band-stop, high-pass, and band-pass filters is presented in [21], employing similar DGS techniques. As discussed in [22], advanced isolation techniques, such as those using composite mode co-planar waveguide structures, have also shown promise in enhancing isolation in dual-band filters for 5th Generation (5G) and body-centric applications. Authors of [23] explored the design of an mm-wave antenna for 5G communications, employing MIMO technology (utilizing slot/slots-etching approaches). The significance of reducing MC in next-generation wireless communication systems is emphasized in their study. In [24, 25] a comprehensive review of techniques for MC reduction in MIMO antennas is conducted, particularly focusing on the effectiveness of DGS and parasitic elements. Furthermore, the authors of [26] undertook a thorough examination of MC in collocated dipole antenna setups, highlighting its impact and discussing potential strategies for mitigation. Refs. [27–29] underscore the significance of advanced feed network designs in mitigating MC issues. An efficient Substrate Integrated Waveguide (SIW) feeding network for suppressing MC in slot array antenna is proposed in [27], thereby enhancing overall array performance. Similarly, in [28] a miniaturized and broadband array antenna with an efficient hybrid feed network is developed, demonstrating improved radiation characteristics and reduced MC effects. Moreover, [29] presents a high-gain and high-isolation SIW MIMO antenna using orthogonal diversity for increasing isolation between the radiating elements. Decoupling and matching networks are recognized as efficient solutions for reducing MC. In [30], a decoupling and matching network design is implemented for a MIMO handset antenna, providing valuable insights into enhancing antenna isolation and performance. Ref. [31] introduces a suitable matching and decoupling network design customized for single/dual-band two-element array antennas, aiming to optimize their performance by minimizing MC. Moreover, [18] applies a decoupling method to enhance element isolation in a dual-band array antenna, thereby improving the overall performance and reliability of the array. In [32], a 12 dB improvement in MC between two elements of a microstrip array has been achieved using a split ring resonator. Ref. [33] introduces a compressed planar monopole array with a neutralization line for UWB communications, offering improved performance and reduced MC effects. In [34], a circuit known as multipath decoupling is proposed to effectively decouple a double-band MIMO receiver within a compact dimension. Furthermore, in [35] additional networks are introduced on top of MIMO antennas to mitigate coupling effects and equalize operating bandwidths. Authors of [36] investigated MC reduction in array antenna using L-loading E-shaped electromagnetic band gap structures, aiming to enhance the isolation between array elements. Moreover, innovations in fully isolated three-port converter designs have also contributed to advancements in decoupling methodologies, showcasing their

utility in managing electrical isolation and mitigating coupling effects in diverse applications [37]. Generally, the presence of significant MC can result in various challenges, including degradation of spatial and pattern diversity, poor isolation between antenna ports, reduction in antenna gain and efficiency, and the emergence of a strong correlation among radiator elements [38, 39]. Structures with specific aperture distributions are commonly employed in radar and military applications. In such scenarios, certain elements are considered in the design of broadband aperture coupling microstrip array antenna, aiming to achieve directional radiation patterns and minimize side-lobe levels. Moreover, the Taylor distribution is utilized for the appropriate allocation of power to individual elements within the antenna network, thereby enhancing the overall performance [40]. The effectiveness of the mentioned MC reduction techniques in enhancing the gain and bandwidth of a bi-layer beam-scanning array antenna is observed. Researchers developed a two-layer beam-scanning array antenna with an improved Butler matrix-feeding network, while in [41], emphasis is placed on improving the Butler matrix features for a mm-wave beam-steering array antenna. Additionally, proper insulation within the structure is ensured by these techniques, and the dimensions of the structure are densified, resembling body-centric systems [42–44]. As previously mentioned, there are numerous methods available for reducing MC phenomena. In this paper, the utilization of a neutralization line is presented as a novel approach to diminish the adverse effects of element coupling in a dual-element array antenna configuration. The strategic placement of a neutralization line between two active elements redirects surface currents away from adjacent elements, effectively reducing MC. Moreover, WOA is used to find the optimized dimensions for the proposed neutralization line which minimize the S_{21} , maximize the gain, and maintain the S_{11} under -10 dB. Notably, this innovative structure is designed to achieve ultra-wide bandwidth characteristics of 1.2 GHz within the ISM band (2.4–2.8 GHz). ISM band is one of the main standard frequency bands for biotelemetry applications. The results show that the proposed structure can be used for biotelemetry applications. The key innovations of this research can be summarized as follows:

- A highly effective technique for reducing MC has been implemented, resulting in a more efficient and compact antenna array, further enhanced through optimization with the WOA.
- An impressive 27 dB reduction in MC was achieved, making the design especially suitable for MIMO applications.
- A new coupling reduction segment was introduced, ensuring that the primary radiation properties remained intact.
- An optimized neutralization line was designed to redirect surface currents back to the radiating element, significantly reducing leakage to adjacent elements. The dimensions of this line were obtained using WOA for better performance.

The subsequent sections of the article are described as follows. Section 2 introduces the initial antenna design, while

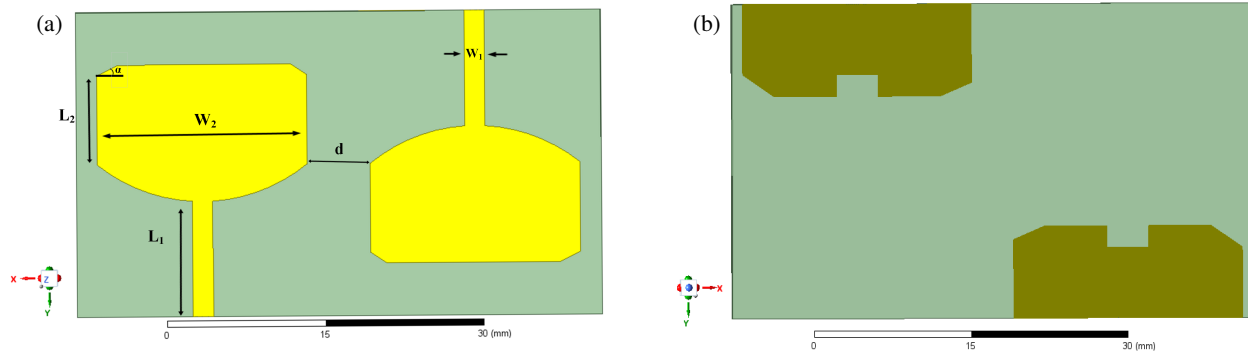


FIGURE 1. Planned microstrip array antennas: (a) Top view, (b) Back view.

Section 3 presents the optimized neutralization line structure and demonstrates its effect on reducing MC. Section 4 compares the experimental results with the computer simulations to highlight the effectiveness of the proposed design. The concluding section summarizes the key findings and implications of the study.

2. GEOMETRY OF THE ARRAY ANTENNA

This section introduces the geometry of the suggested microstrip array antenna. Initially, a microstrip array antenna with two elements is proposed. It is worth noting that various structures have been evaluated. Ultimately, an array antenna operating in the standard ISM band was designed. The microstrip structure was chosen due to its unique properties and flexibility, which facilitate the design of the desired array. An array with two microstrip antennas was designed and implemented to achieve a wide bandwidth in the ISM band and an omnidirectional radiation pattern. The proposed structure is depicted in Fig. 1. The antenna dimensions are as follows: $W_1 = 2\text{ mm}$, $W_2 = 20\text{ mm}$, $L_1 = 10\text{ mm}$, $L_2 = 12\text{ mm}$, $\alpha = 27^\circ$, and $d = 2\text{ mm}$.

The substrate of this structure is defined as an FR4 microstrip patch array with a relative permittivity of 4.4 with 1.6 mm thickness, and the structure size is $50\text{ mm} \times 30\text{ mm} \times 1.6\text{ mm}$. Furthermore, an incomplete ground structure is suggested to achieve the optimal bandwidth. The minimum possible distance between the elements is chosen to minimize alterations in the main radiation properties. Subsequently, a coupling reduction element will be added to suppress the MC between the antenna elements.

MC is the energy absorbed by an adjacent element when the antenna radiates. This parameter can alter the radiation pattern, input impedance, and return loss of MIMO antennas. Fig. 2 shows the model of the equivalent circuit for the planned geometry displayed in Fig. 1.

Thus, the following simple circuit equations can be used to analyze the model [26]:

$$\begin{aligned} V_1 &= Z_{11}I_1 + Z_{12}I_2, \\ V_2 &= Z_{21}I_1 + Z_{22}I_2. \end{aligned} \quad (1)$$

If antenna 1 is in transmitting mode, i.e., $I_1 \neq 0$ and $I_2 = 0$, then voltage V_2 is the induced voltage due to the current I_1

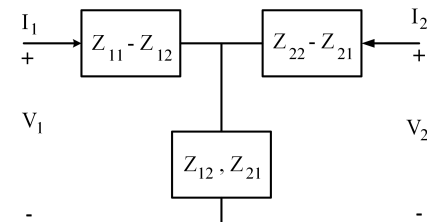


FIGURE 2. T-Network Equivalent.

at the location of antenna 2. This induction effect in the adjacent element is known as MC. If the mutual impedance between the elements, i.e., Z_{12} and Z_{21} , is zero (in a symmetric array $Z_{12} = Z_{21}$), the MC will be zero. Typically, the MC between elements i and j is assumed to be proportional to the parameter S between the corresponding elements. Considering an array with two elements, let's denote its scattering matrix $[S]$. S_{ij} ($i \neq j$) indicates the MC, which ideally should be $S_{ij}(i \neq j) = 0$ for $i, j = 0, 1, 2, 3, \dots$. In this case, the array elements would operate independently, demonstrating the best radiation characteristics. However, achieving a zero value for the scattering parameter on the off-diagonal elements of the scattering matrix is not feasible in practice. Therefore, by altering the structure, reducing this value as close to zero as possible will significantly minimize the coupling between elements.

As observed in Fig. 3, when the minimum distance between two elements is changed from 2 to 9 mm, the behavior of the S parameter will change.

These results demonstrate that the distance between elements plays a crucial role in the MC within the array. Increasing the

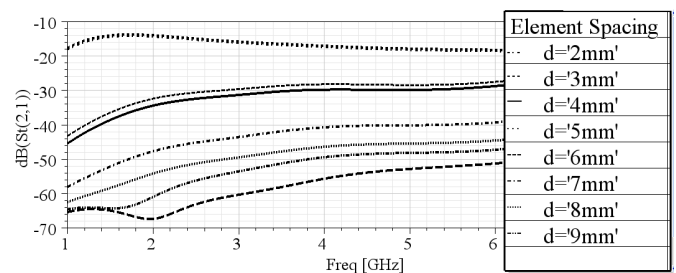


FIGURE 3. Simulation results coupling S-parameter variations for different element spacing.

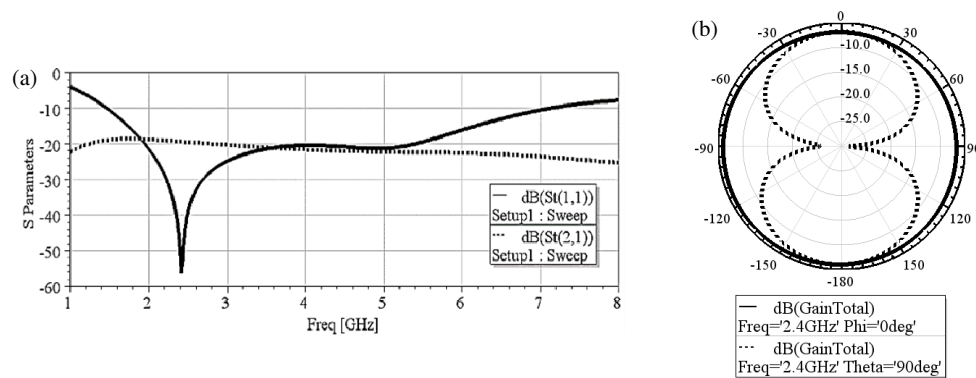


FIGURE 4. The simulation outcomes of the proposed array antenna at 2.4 GHz: (a) Scattering parameter analysis, (b) Radiation pattern analysis.

distance between elements reduces MC; however, it also results in a larger array size, which is not ideal for low-profile structures. Therefore, to demonstrate the efficiency of the suggested method in this article, we have intentionally selected an inter-element spacing that results in significant MC. The proposed method is then applied to mitigate this coupling. As can be observed, the maximum coupling occurred for $d = 2$ mm.

Generally, in Fig. 4, the simulation's outcome of the scattering parameter and radiation patterns are depicted. The radiation patterns of the designed antenna are nearly omnidirectional with a maximum gain of -6.17 dB at 2.4 GHz. Furthermore, a bandwidth of 5.7 GHz is achieved by the structure and $f_0 = 2.4$ GHz. An MC of -19 dB is obtained at f_0 . It is essential to note that these values will serve as the benchmark for evaluation after applying the proposed method and reducing MC.

As previously mentioned, the distance between adjacent elements plays a crucial role in MC. The calculated current distributions on the antenna surface and the dielectric's top plate are depicted in Fig. 5 for $d = 2$ mm.

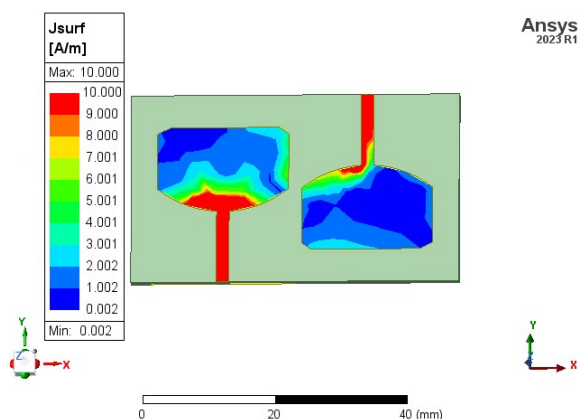


FIGURE 5. The current distribution of the proposed antenna at 2.4 GHz.

The surface currents at 2.4 GHz strongly flow toward the other port, inducing current to propagate towards the opposite port, resulting in a wave propagation from the off port. Minimizing leakage current flow on the surface is crucial to efficiently reduce coupling. To mitigate the adverse effects of sur-

face current, one approach is to place a dummy element or two elements where the surface current dissipates. Another method is to guide the surface current towards the radiating element by placing a neutralization line. For this reason, the optimal structure will be introduced in the next section.

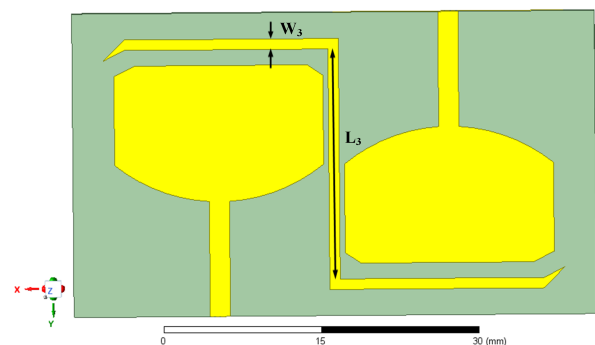


FIGURE 6. The proposed structure with a decoupling segment.

3. THE PROPOSED MODIFIED STRUCTURE WITH OPTIMIZATION PROCESS

As previously observed in Fig. 5, the primary leakage of current from one element to another occurs through the transmission line and surface currents on the upper dielectric layer. Therefore, a crank-shape neutralization line is proposed to reduce the effect of surface current as shown in Fig. 6. This neutralization line effectively reduces the surface current's impact, preventing the leakage and induced currents from the first element from affecting the adjacent one. Furthermore, to minimize the negative impact of surface current leakage on the array's radiation characteristics, an additional element is integrated at the end of the neutralization line. This element helps guide the surface current back towards the radiating element, ensuring that the radiation performance is not compromised. To fine-tune the dimensions of L_3 and W_3 , WOA is applied, optimizing these parameters for the best possible performance.

3.1. Neutralization Line Optimization and Impact

Incorporating the neutralization line is expected to significantly decrease the mutual coupling between the antennas by prevent-

ing unwanted current leakage to the adjacent element. However, it is vital to determine the optimum dimensions for L_3 and W_3 . For this reason, the WOA is utilized [45]. The objective function was designed to minimize S_{21} (coupling between antenna elements), maximize the gain, and ensure that S_{11} (input reflection coefficient) remained below -10 dB. The weighted fitness function was formulated as below:

$$\text{Fitness} = w_1 \cdot S_{21} - w_2 \cdot \text{Gain} + w_3 \cdot P_{S_{11}} \quad (2)$$

where,

$$P_{S_{11}} = \begin{cases} \mu \cdot (S_{11} + 10)^2 & \text{if } S_{11} > -10 \text{ dB} \\ 0 & \text{otherwise} \end{cases} \quad (3)$$

Moreover, w_1 , w_2 , and w_3 are weights assigned to S_{21} , gain, and the penalty term ($P_{S_{11}}$), respectively, to control their relative importance in the optimization process. The values of these weights are considered as: $w_1 = 1$, $w_2 = 0.3$, and $w_3 = 0.7$ since the reduction of S_{21} is more important. Also, μ is a large penalty coefficient that ensures that the constraint on S_{11} is strictly enforced and is set to 100. The WOA begins by generating an initial population of whales distributed randomly within the design space as can be seen in Fig. 7.

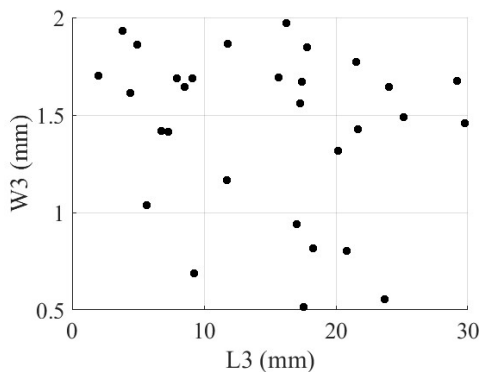


FIGURE 7. Population Distribution at First Iteration.

For each iteration, the design parameters L_3 and W_3 for all candidates are exported to High Frequency Structure Simulator (HFSS), where the antenna model is simulated to evaluate key performance metrics such as S_{21} , S_{11} , and gain. These metrics are then sent back to MATLAB, where the fitness value for each candidate solution is calculated using the objective function (2). Based on the fitness values, the WOA updates the positions of the whales using encircling, spiral, and random search mechanisms. The updated parameters are subsequently sent back to HFSS for further evaluation. This iterative process continues until the algorithm converges, providing optimal dimensions for the neutralization line that significantly reduces mutual coupling, enhances gain, and maintains $S_{11} < -10$ dB. The flowchart of the optimization process used in this paper is presented in Fig. 8.

The boundary constraints for L_3 and W_3 are considered $[1, 30]$ mm and $[0.5, 2]$ mm, respectively, to align with the real dimensions of the proposed array antenna. The population size is set to 30, and the total number of iterations is defined as 50

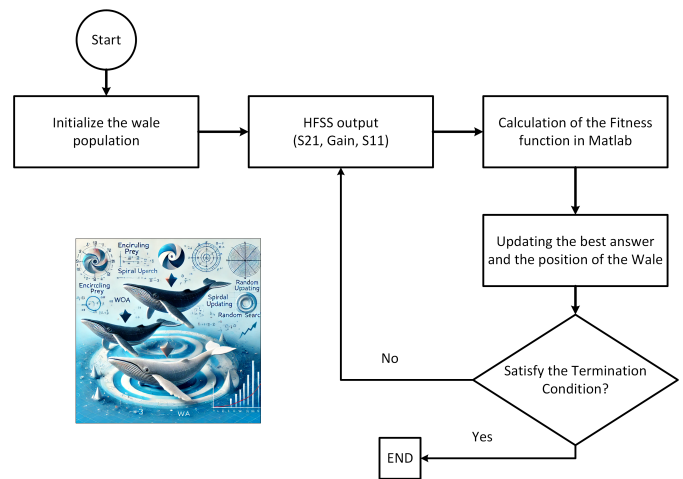


FIGURE 8. Flowchart of the utilized optimization process.

to achieve the optimized solution. Fig. 9 shows the final distribution of the whale population at the last iteration. As seen, the optimal point (red point) for the (L_3, W_3) is $(23, 1)$ mm. Moreover, the convergence curve of the WOA is shown in Fig. 10. As shown, the algorithm progressively reduces the fitness value with each iteration, demonstrating that the population of whales is continuously converging toward the optimal solution.

The current distribution on the antenna surfaces and the top plate of the dielectric are presented in Fig. 11, for the optimal solution $(L_3, W_3) = (23, 1)$ mm.

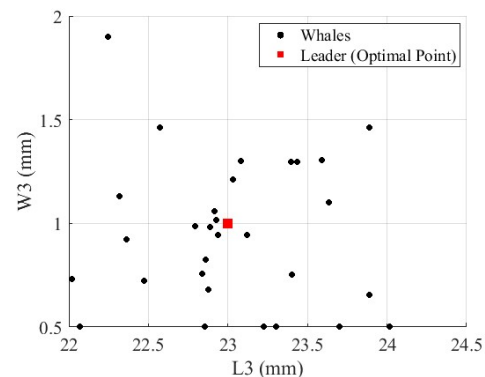


FIGURE 9. Final distribution of the whales population.

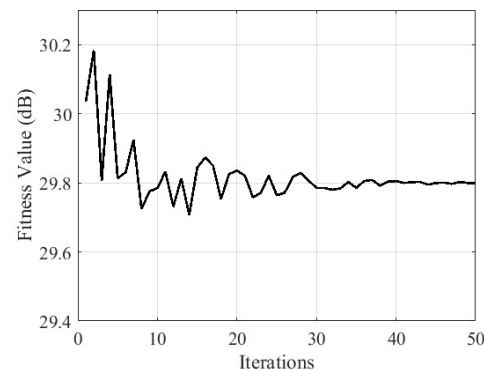


FIGURE 10. Convergence of WOA.

TABLE 1. Comparison of suggested MC reduction with other published researches.

Ref.	Year	Element Spacing (λ_0)	S_{21} (dB)	Array	Coupling Reduction Method
This Paper	2024	0.16	-27	1×2	WOA-optimized Neutralization Line Adding
[46]	2024	0.16	-22 (2.45 GHz), -27 (5.4 GHz)	1×2	Parasitic Element Adding (Dual Bands)
[35]	2023	0.03	-21	1×2	Near Field Coupling Reduction
[18]	2022	0.78	-10	1×2	Decoupling and Matching Network
[40]	2021	0.15	-23	1×2	Decoupling and Matching Network
[31]	2020	2	-31	1×2	Decoupling and Matching Network
[47]	2017	0.83	-16	1×2	Metamaterial
[48]	2017	0.08	-30	1×2	Array-Antenna Decoupling Surface
[36]	2016	0.26	-26	1×2	Electromagnetic Band Gap
[49]	2016	0.72	-20	7×3	Asymmetrical Coplanar Strip Wall
[50]	2014	0.05	< -40	1×2	Slot-Combined Complementary Split Ring Resonators
[51]	2011	0.50	< -20	1×2	Folded Split-Ring Resonators
[52]	2011	0.72	< -20	7×3	Metamaterial

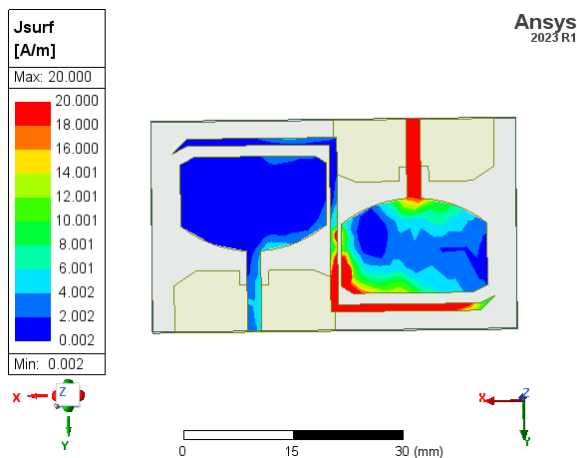
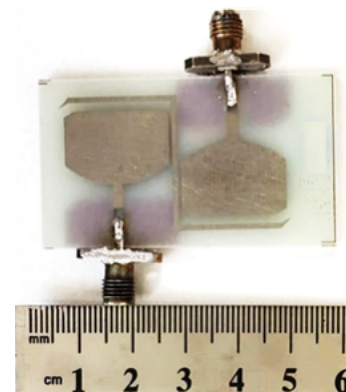
**FIGURE 11.** Current distribution of the modified antennas at 2.4 GHz.**FIGURE 12.** The fabricated antenna.

Figure 11 clearly shows that at 2.4 GHz, the neutralization line effectively prevents current leakage to the adjacent element and ultimately even redirects the current back to the radiating element. This is a confirmation of the positive effect of the proposed method in reducing MC with the comparison of Fig. 5.

4. EXPERIMENTAL RESULTS

To validate the accuracy of the software design results, an antenna prototype has been manufactured and measured under real conditions, as depicted in Fig. 12. The substrate of the structure is FR4 with a thickness of 1.6 mm.

The measurement outcomes demonstrate the effectiveness of this methodology on practical antennas, as shown in Fig. 13. The empirical findings support the simulation results, confirm-

ing the desired accuracy of the method. It is worth mentioning that the measured outcomes of the scattering parameters (rather than the frequency response of the structure) differ slightly from the simulations. This discrepancy can be attributed to testing conditions such as the connected connector and fabrication precision. The MC is approximately -27 dB; the bandwidth is about 1.2 GHz; and the peak gain is -5.19 dB.

In Table 1, the results of the suggested decoupling method have been compared with results from other reported researches with different coupling reduction methods. Consequently, the technique proposed in this paper effectively suppresses the MC phenomena and offers compact structures suitable for certain aperture distributions, such as Taylor or Chebyshev distributions. Moreover, the proposed technique can be applied to in-body array antennas, reducing the overall dimensions of the structure.

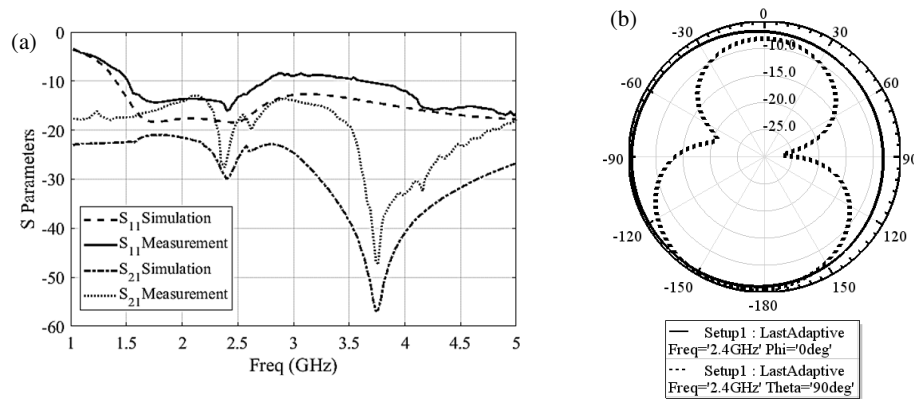


FIGURE 13. The measurement results of the antenna prototype, (a) S -parameters results (simulation and measurement), (b) Radiation pattern results at 2.4 GHz.

5. CONCLUSION

In this paper, a decoupling technique is introduced to reduce mutual coupling in UWB array antennas. The method involves incorporating a passive neutralization line between two patches to suppress coupling effects. This neutralization line is strategically placed to redirect leaky currents back to the radiating element, preventing their leakage to adjacent elements while maintaining the antenna's central frequency and radiation pattern. The dimensions of the neutralization line are optimized using WOA to achieve the best possible performance, focusing on minimizing mutual coupling and enhancing gain. The proposed antenna design achieves an ultra-wide bandwidth of 1.2 GHz within the ISM band, with a significant 27 dB reduction in mutual coupling at the central frequency of 2.4 GHz and a maximum gain of -5.19 dB. Simulation results and experimental measurements confirm that the optimized design is effective, with the fabricated antenna performing as expected. This simple yet powerful design approach, leveraging WOA, offers strong potential for compact and efficient applications in the specified frequency band and can be extended to other antenna array configurations.

REFERENCES

- [1] Fakharian, M. M. and P. Rezaei, "Very compact palmate leaf-shaped CPW-FED monopole antenna for UWB applications," *Microwave and Optical Technology Letters*, Vol. 56, No. 7, 1612–1616, 2014.
- [2] Jing, D. and H. Li, "A compact dual-band two-element implantable MIMO antenna for biotelemetric applications," in *2022 IEEE MTT-S International Microwave Workshop Series on Advanced Materials and Processes for RF and THz Applications (IMWS-AMP)*, 1–3, Guangzhou, China, 2022.
- [3] Hatam, M., A. Sheikhi, and M. A. Masnadi-Shirazi, "A pulse-train MIMO radar based on theory of independent component analysis," *Iranian Journal of Science and Technology, Transactions of Electrical Engineering*, Vol. 35, 75–94, 2011.
- [4] Dalakoti, N. and P. Jain, "A compact dual-element UWB-MIMO antenna with single band-notched characteristics," *Frequenz*, Vol. 23, 335–345, 2024.
- [5] Nasrabadi, E. and P. Rezaei, "A novel design of reconfigurable monopole antenna with switchable triple band-rejection for UWB applications," *International Journal of Microwave and Wireless Technologies*, Vol. 8, No. 8, 1223–1229, 2016.
- [6] Mohammadi, B., A. Valizade, J. Nourinia, and P. Rezaei, "Design of a compact dual-band-notch ultra-wideband bandpass filter based on wave cancellation method," *IET Microwaves, Antennas & Propagation*, Vol. 9, No. 1, 1–9, 2015.
- [7] Khani, S., M. Danaie, P. Rezaei, and A. Shahzadi, "Compact ultra-wide upper stopband microstrip dual-band BPF using tapered and octagonal loop resonators," *Frequenz*, Vol. 74, No. 1–2, 61–71, 2020.
- [8] Dadashzadeh, G., E. Jedari, M. Hakak, and M. Kamareei, "Antenna array configuration effects on the radiation pattern and BER of the modified adaptive CMA in CDMA based systems," *Iranian Journal of Science & Technology, Transaction B, Engineering*, Vol. 30, 277–284, 2006.
- [9] Nimehvari Varcheh, H. and P. Rezaei, "Integration of the modified butler matrix and decoupling network for beam-steering antenna array," *International Journal of RF and Microwave Computer-Aided Engineering*, Vol. 32, No. 3, e23015, 2022.
- [10] Bijanmanesh, M., N. Etesami, and R. Darvishi, "Analysis of slot-coupled, ridged-circular disk microstrip antenna element using the cavity model," *Iranian Journal of Science and Technology, Transactions of Electrical Engineering*, Vol. 25, 499–508, 2001.
- [11] Sohi, A. K. and A. Kaur, "Slot and SRR-loaded quad-port, hen-shaped fractal UWB-MIMO antenna with quad band-reject ability for handheld 4G/5G wireless devices," *Iranian Journal of Science and Technology, Transactions of Electrical Engineering*, Vol. 47, No. 3, 1187–1205, 2023.
- [12] Alfakhri, A., "Dual polarization and mutual coupling improvement of UWB MIMO antenna with cross shape decoupling structure," *E-Prime — Advances in Electrical Engineering, Electronics and Energy*, Vol. 4, 100130, Jun. 2023.
- [13] Dama, Y. A. S., R. A. Abd-Alhameed, S. M. R. Jones, D. Zhou, N. J. McEwan, M. B. Child, and P. S. Excell, "An envelope correlation formula for (N, N) MIMO antenna arrays using input scattering parameters, and including power losses," *International Journal of Antennas and Propagation*, Vol. 2011, No. 1, 421691, 2011.
- [14] Fakharian, M. M. and P. Rezaei, "Mutual coupling reduction in microstrip array antenna using a novel compact electromagnetic band-gap structure," in *2nd National Conference New Technolo-*

- gies in *Electrical and Computer Engineering*, 1–9, 2019.
- [15] Khani, S., M. Danaie, and P. Rezaei, “Compact and low-power all-optical surface plasmon switches with isolated pump and data waveguides and a rectangular cavity containing nano-silver strips,” *Superlattices and Microstructures*, Vol. 141, 106481, 2020.
 - [16] Tunio, I. A., Y. Mahe, T. Razban-Haghighi, and B. Froppier, “Mutual coupling reduction in patch antenna array using combination of shorting pins and metallic walls,” *Progress In Electromagnetics Research C*, Vol. 107, 157–171, 2021.
 - [17] Habibi Daronkola, A., F. T. Hamedani, P. Rezaei, and N. Montaseri, “Mutual coupling reduction using plane spiral orbital angular momentum electromagnetic wave,” *Journal of Electromagnetic Waves and Applications*, Vol. 36, No. 3, 346–355, 2022.
 - [18] Atashpanjeh, E. and P. Rezaei, “Applying decoupling method to a dual-band antenna array for element isolation,” *Modeling and Simulation in Electrical and Electronics Engineering*, Vol. 1, No. 4, 1–5, 2022.
 - [19] Zhao, L., L. Liu, and Y.-M. Cai, “A MIMO antenna decoupling network composed of inverters and coupled split ring resonators,” *Progress In Electromagnetics Research C*, Vol. 79, 175–183, 2017.
 - [20] Wang, Z., Z. Wang, H. Liu, and S.-J. Fang, “Differential negative group delay circuit topology with reverse nested double U-shaped defected ground structure,” *Progress In Electromagnetics Research C*, Vol. 132, 65–77, 2023.
 - [21] Yuan, W., X. Liu, H. Lu, W. Wu, and N. Yuan, “Flexible design method for microstrip bandstop, highpass, and bandpass filters using similar defected ground structures,” *IEEE Access*, Vol. 7, 98 453–98 461, 2019.
 - [22] Bhat, Z. A., J. A. Sheikh, S. D. Khan, I. Bashir, and S. A. Parah, “A new method of isolation enhancement of dual band band-pass filter using composite mode co-planar waveguide structure for 5G and body centric applications,” *Iranian Journal of Science and Technology, Transactions of Electrical Engineering*, Vol. 47, No. 1, 317–326, 2023.
 - [23] Devi, B. R., C. Niharika, A. M. Lakshmi, D. Jayaram, and B. Tarun, “Design of a millimeter wave antenna using MIMO for 5G applications,” in *2021 IEEE 2nd International Conference on Applied Electromagnetics, Signal Processing, & Communication (AESPC)*, 1–7, Bhubaneswar, India, 2021.
 - [24] Kumar, A., A. Q. Ansari, B. K. Kanaujia, J. Kishor, and L. Matekovits, “A review on different techniques of mutual coupling reduction between elements of any MIMO antenna. Part 1: DGSs and parasitic structures,” *Radio Science*, Vol. 56, No. 3, 1–25, 2021.
 - [25] Elalaouy, O., M. E. Ghzaoui, and J. Foshi, “Mutual coupling reduction of a two-port MIMO antenna using defected ground structure,” *E-Prime — Advances in Electrical Engineering, Electronics and Energy*, Vol. 8, 100557, Jun. 2024.
 - [26] Adesoye, A. S., J. J. Popoola, and A. O. Fadamiro, “Mutual coupling in a collocated dipole antenna setup: A comprehensive review,” *Journal of Multidisciplinary Engineering Science and Technology (JMEST)*, Vol. 8, 2458–9403, 2022.
 - [27] Khatami, S. A., J. Meiguni, A. A.-e. Elahi, and P. Rezaei, “Compact via-coupling fed monopulse antenna with orthogonal tracking capability in radiation pattern,” *IEEE Antennas and Wireless Propagation Letters*, Vol. 19, No. 8, 1443–1446, 2020.
 - [28] Karami, F., P. Rezaei, A. Amn-e Elahi, and J. S. Meiguni, “A compact and wideband array antenna with efficient hybrid feed network,” *International Journal of RF and Microwave Computer-Aided Engineering*, Vol. 30, No. 11, e22393, 2020.
 - [29] Pant, M. and L. Malviya, “SIW MIMO antenna with high gain and isolation for fifth generation wireless communication systems,” *Frequenz*, Vol. 78, No. 9-10, 479–497, 2024.
 - [30] Kormilainen, R., R. Luomaniemi, A. Lehtovuori, and V. Viikari, “A lumped-element decoupling and matching network for a four-element mobile handset MIMO antenna,” *International Journal of Antennas and Propagation*, Vol. 2019, No. 1, 1934726, 2019.
 - [31] Xu, K.-D., H. Luyen, and N. Behdad, “A decoupling and matching network design for single-and dual-band two-element antenna arrays,” *IEEE Transactions on Microwave Theory and Techniques*, Vol. 68, No. 9, 3986–3999, 2020.
 - [32] Bharath, S., S. Bharath, Sunil, K. S. Iranna, and H. Santoshkumar, “A novel design of modified split ring resonator for reduction of mutual coupling in microstrip patch antenna array,” *International Journal of Science Technology and Engineering*, Vol. 11, 34–37, 2018.
 - [33] Yu, Y., X. Liu, Z. Gu, and L. Yi, “A compact printed monopole array with neutralization line for UWB applications,” in *2016 IEEE International Symposium on Antennas and Propagation (APSURSI)*, 1779–1780, Fajardo, PR, USA, 2016.
 - [34] Singh, H. V., D. V. S. Prasad, and S. Tripathi, “Dual-band MIMO antenna decoupling using vias based multipath decoupling circuit,” *Microwave and Optical Technology Letters*, Vol. 64, No. 4, 770–777, 2022.
 - [35] Omidvar, A., P. Rezaei, and E. Atashpanjeh, “Mutual coupling reduction with Peyton Turtle pattern nearfield surface for MIMO patch antenna,” *Frequenz*, Vol. 77, No. 7-8, 395–401, 2023.
 - [36] Jiang, T., T. Jiao, and Y. Li, “Array mutual coupling reduction using L-loading E-shaped electromagnetic band gap structures,” *International Journal of Antennas and Propagation*, Vol. 2016, No. 1, 6731014, 2016.
 - [37] Mobarak, M., M. Saradarzadeh, and I. Pourfar, “Design of an innovative structure for DC electric spring based on fully isolated three-port converter,” *Iranian Journal of Science and Technology, Transactions of Electrical Engineering*, Vol. 48, 847–857, 2024.
 - [38] Wu, W.-J., Y.-F. Cheng, S. Chen, C. Wei, and G. Wang, “Decoupling and bandwidth equalization for MIMO antennas by using novel network design,” *Microwave and Optical Technology Letters*, Vol. 64, No. 8, 1462–1467, 2022.
 - [39] Chen, K.-H. and J.-F. Kiang, “Effect of mutual coupling on the channel capacity of MIMO systems,” *IEEE Transactions on Vehicular Technology*, Vol. 65, No. 1, 398–403, 2016.
 - [40] Abesht, M., N. A. Tinat, and H. Oraizi, “Design and simulation of array antenna in ku band with high gain and very low sidelobe level for space and radar applications,” *Radar*, Vol. 8, No. 2, 79–88, 2020.
 - [41] Razi, Z. M. and P. Rezaei, “A two-layer beam-steering array antenna with 4×4 modified Butler matrix fed network for switched beam application,” *International Journal of RF and Microwave Computer-Aided Engineering*, Vol. 30, No. 2, e22028, 2020.
 - [42] Mousavi, Z. and P. Rezaei, “Millimetre-wave beam-steering array antenna by emphasising on improvement of butler matrix features,” *IET Microwaves, Antennas & Propagation*, Vol. 13, No. 9, 1287–1292, 2019.
 - [43] Atashpanjeh, E. and A. Pirhadi, “Design of wideband monopole antenna loaded with small spiral for using in wireless capsule endoscopy systems,” *Progress In Electromagnetics Research C*, Vol. 59, 71–78, 2015.
 - [44] Atashpanjeh, E. and P. Rezaei, “Broadband conformal monopole antenna loaded with meandered arms for wireless capsule endoscopy,” *Wireless Personal Communications*, Vol. 110, No. 4, 1679–1691, 2020.

- [45] Gharehchopogh, F. S. and H. Gholizadeh, "A comprehensive survey: Whale optimization algorithm and its applications," *Swarm and Evolutionary Computation*, Vol. 48, 1–24, 2019.
- [46] Awan, W. A., T. Islam, F. N. Alsunaydih, F. Alsaleem, and K. Alhassoonc, "Dual-band MIMO antenna with low mutual coupling for 2.4/5.8 GHz communication and wearable technologies," *PLOS One*, Vol. 19, No. 4, e0301924, Apr. 2024.
- [47] Zhu, X., X. Yang, Q. Song, and B. Lui, "Compact UWB-MIMO antenna with metamaterial FSS decoupling structure," *EURASIP Journal on Wireless Communications and Networking*, Vol. 2017, 1–6, 2017.
- [48] Wu, K.-L., C. Wei, X. Mei, and Z.-Y. Zhang, "Array-antenna decoupling surface," *IEEE Transactions on Antennas and Propagation*, Vol. 65, No. 12, 6728–6738, Dec. 2017.
- [49] Qi, H., L. Liu, X. Yin, H. Zhao, and W. J. Kulesza, "Mutual coupling suppression between two closely spaced microstrip antennas with an asymmetrical coplanar strip wall," *IEEE Antennas and Wireless Propagation Letters*, Vol. 15, 191–194, 2015.
- [50] Qamar, Z., L. Riaz, M. Chongcheawchamnan, S. A. Khan, and M. F. Shafique, "Slot combined complementary split ring resonators for mutual coupling suppression in microstrip phased arrays," *IET Microwaves, Antennas & Propagation*, Vol. 8, No. 15, 1261–1267, 2014.
- [51] Habashi, A., J. Nourinia, and C. Ghobadi, "Mutual coupling reduction between very closely spaced patch antennas using low-profile folded split-ring resonators (FSRRs)," *IEEE Antennas and Wireless Propagation Letters*, Vol. 10, 862–865, 2011.
- [52] Tang, M.-C., S. Xiao, B. Wang, J. Guan, and T. Deng, "Improved performance of a microstrip phased array using broadband and ultra-low-loss metamaterial slabs," *IEEE Antennas and Propagation Magazine*, Vol. 53, No. 6, 31–41, 2011.